MAGNETOHYDRODYNAMICS Vol. 37 (2001), No. 1-2, pp. 112–118

Flow driven by Marangoni convection and Rotating Magnetic Field in a Floating-Zone configuration

L. Martin Witkowski, J.S. Walker

Department of Mechanical and Industrial Engineering, University of Illinois, 1206 W. Green St., Urbana, IL 61801, USA

This paper treats the axisymmetric flow driven by Marangoni convection and a Rotating Magnetic Field (RMF) in a Floating-Zone configuration. For a low Prandtl number liquid, and different Marangoni values, we investigate the evolution of the flow as the intensity of the RMF is increased. It evolves from a Marangoni dominated flow to a RMF dominated flow. We particularly emphasise and explain the transition region where both sources of motion surprisingly tend to cancel each other.

Introduction Float-Zone is the method of choice to produce high-purity silicon crystals. A polycrystalline rod is moved through a heater. As the melt solidifies on a crystal seed a single crystal grows. This containerless technique yields dislocation-free crystal. The presence of thermally induced surface tension gradients along the free surface leads to a strong convection (called Marangoni convection) in the melt that produces undesirable macro and microsegregation. A drastic reduction of microsegregation due to a rotating magnetic field (RMF) in a crystal grown with floating-zone technique has been shown experimentally [1]. The effect of the RMF is to produce a prescribed azimuthal body force in the melt. In the experiments [1], the flow is in a regime where realistic numerical simulation is still difficult to achieve. We study a simplified situation to understand some of the mechanisms that occur when the flow is driven by both sources of motion.

The classical model for the study of Marangoni convection in a liquid bridge is to consider the liquid suspended between two planar circular isothermal disks at different temperature [2], [3]. The buoyant convection is usually neglected when compared to the Marangoni convection. This situation is often referred to as a half-zone. While the free-surface position is not known a-priori, a further simplification is to consider its location to be at a constant radius. In our study, we keep most of half-zone simplifications with the notable exception that we take both disks to be at melting temperature and a heat flux is prescribed along the free surface. Such models have already been proposed [4], [5], [6]. We use the same parabolic expression for the heat flux as the latter.

1. Problem formulation We use cylindrical coordinates r, θ, z with the $z-$axis along the centerline of the cylinder with the origin at the middle of the liquid region and unit vectors $\boldsymbol{e}_r, \boldsymbol{e}_\theta, \boldsymbol{e}_z$. The free surface is located at a radius R^* and we fix the distance between the feed rod and the crystal at $2R^*$.

We make the assumption that the flow remains axisymmetric and steady. We normalize length by R^* and velocity by ν/R^*, where ν is the kinematic viscosity of the fluid. We use the vorticity $\Omega \cdot \boldsymbol{e}_\theta = \nabla \wedge \boldsymbol{V}$, stream-function ψ formulation where $\nabla \wedge (-\frac{\psi}{r} \cdot \boldsymbol{e}_\theta) = (u_r, 0, u_z)$ and the velocity $\boldsymbol{V} = (u_r, u_\theta, u_z)$. We introduce the

angular momentum $\Gamma = ru_\theta$. The Navier-Stokes equations are

$$\frac{\partial(u_r\Omega)}{\partial r} + \frac{\partial(u_z\Omega)}{\partial z} - \frac{\partial}{\partial z}\left(\frac{\Gamma^2}{r^3}\right) = \frac{\partial^2\Omega}{\partial r^2} + \frac{1}{r}\frac{\partial\Omega}{\partial r} - \frac{\Omega}{r^2} + \frac{\partial^2\Omega}{\partial z^2}, \tag{1}$$

$$\frac{\partial^2\psi}{\partial r^2} - \frac{1}{r}\frac{\partial\psi}{\partial r} + \frac{\partial^2\psi}{\partial z^2} = r\Omega, \tag{2}$$

$$\frac{\partial(u_r\Gamma)}{\partial r} + \frac{u_r\Gamma}{r} + \frac{\partial(u_z\Gamma)}{\partial z} = \frac{\partial^2\Gamma}{\partial r^2} - \frac{1}{r}\frac{\partial\Gamma}{\partial r} + \frac{\partial^2\Gamma}{\partial z^2} + Tm \cdot r f_\theta. \tag{3}$$

The Taylor magnetic number *Tm* is $\sigma\omega B^2 R^{*4}/(2\rho\nu^2)$, where ρ is the density and σ is the electrical conductivity of the fluid and B is the intensity of the magnetic field. The RMF is a spatially uniform tranverse field which rotates at an angular velocity ω around the vertical centerline of the cylinder. (Its axial component is zero.) The action of the RMF results in an azimuthal source term in the momentum equation (last term in equation (3)). The body force has an analytical expression [7],

$$f_\theta = r - \frac{\partial\Phi}{\partial z} \text{ where } \Phi = \sum_{n=1}^{\infty} \frac{2J_1(\lambda_n r)\sinh(\lambda_n z)}{\lambda_n(\lambda_n^2 - 1)J_1(\lambda_n)\cosh(\lambda_n)}, \tag{4}$$

is the electrical potential and J_k is the Bessel function of the first kind and kth order, while λ_n are the roots of $\lambda_n J_0(\lambda_n) - J_1(\lambda_n) = 0$. The electrical potential is normalized by $\omega R^{*2} B/2$. In order to calculate the body force, the electric current $\boldsymbol{j}^*$ has been approximated by $-\sigma(\partial \boldsymbol{A}^*/\partial t^* + \nabla\Phi^*)$, where $\boldsymbol{A}^* = (0, 0, A^*)$ is the vector potential of the applied magnetic field $\boldsymbol{B}^*$. We also assumed the induced field due to the currents in the melt to be negligible, which is true as long as the shielding parameter $\mu_p\sigma\omega R^{*2}$ is much less than unity, where the quantity μ_p is the magnetic permeability of the fluid. The body force is taken to be the time average of $\boldsymbol{j}^* \wedge \boldsymbol{B}^*$. The time dependency can be neglected as long as the velocity of the fluid is small compared to ω times R^*. These assumptions are met in almost all crystal-growth experiments.

If the temperature T^* is shifted and normalized so that $T = (T^* - T_S^*)k/(qR^*)$ where T_S^* is the solidification temperature, k is the thermal conductivity and q is the maximum heat flux imposed at the free surface, then the energy equation is

$$\frac{\partial(u_r T)}{\partial r} + \frac{u_r T}{r} + \frac{\partial(u_z T)}{\partial z} = \frac{1}{Pr}\left(\frac{\partial^2 T}{\partial r^2} + \frac{1}{r}\frac{\partial T}{\partial r} + \frac{\partial^2 T}{\partial z^2}\right). \tag{5}$$

The boundary conditions are

$$\psi = \partial\psi/\partial z = \Gamma = T = 0 \text{ at } z = 1$$

and

$$\psi = 0,\ \Omega = (Ma/Pr)\partial T/\partial z,\ \partial\Gamma/\partial r - 2\Gamma/r = 0 \text{ at } r = 1.$$

We use a symmetry condition at $z = 0$. The Prandtl number *Pr* is ν/κ and the Marangoni number *Ma* is $-(\mathrm{d}\gamma/\mathrm{d}\mathrm{T}^*)\mathrm{q}\mathrm{R}^{*2}/(\rho\nu\kappa\mathrm{k})$ where γ is the surface tension and κ the thermal diffusivity of the fluid.

The set of equations and boundary conditions are discretized by a standard second-order accurate finite difference scheme. The steady state solutions are computed using a Newton-Raphson algorithm [3]. The unknowns are properly ordered on each node to form a banded matrix. At each Newton-Raphson iteration, the matrix inversion is done by the routines dgbtrf/dgbtrs taken from the Lapack library. The branches of solutions are computed by a continuation technique. All results presented are performed on a $[r \times z] = [70 \times 90]$ uniform grid.

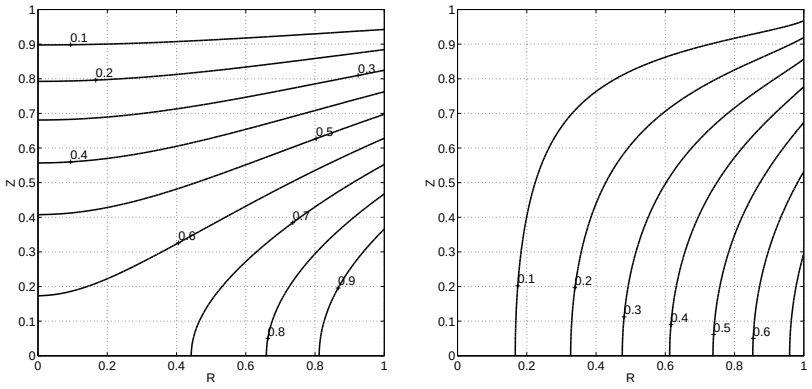

Figure 1: Left : Temperature distribution for the pure diffusive case $Ma = 0$ and $Tm = 0$. Right : Contours of the azimuthal body force due to the RMF.

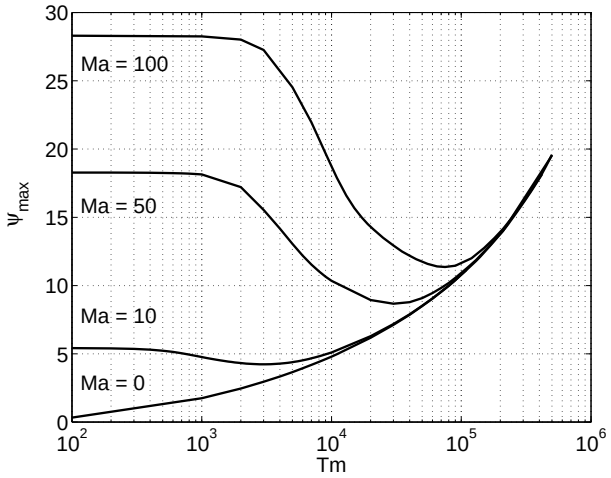

Figure 2: Evolution of ψ_{max} versus *Tm* for $Ma = 0, 10, 50$ and 100 and for $Pr = 0.02$.

2. Results We have set $Pr = 0.02$ which is commonly used for molten semiconductors. The maximum velocities in all results presented here are weak enough that the shape of isotherms are close to the pure conductive case presented in figure 1. The maximum temperature is $T_{max} = 1.06$. The azimuthal body force due to the RMF is also presented in figure 1. The peak value is 0.74 at $r = 1, z = 0$.

When the magnetic field is set to zero ($Tm = 0$), the flow is purely meridional with a counterclockwise cell in $r = [0,1] \times z = [0,1]$. The maximum value of ψ increases with *Ma* and most of the flow is concentrated in the cold corner, [4]. With only the RMF ($Ma = 0$), then we have in addition to an azimuthal motion a meridional counterclockwise cell driven by the axial variation of angular momentum $\partial(\Gamma^2/r^3)/\partial z$ in (1) [8], [9].

We varied parameters in the space $Tm = [0, 5 \cdot 10^5] \times Ma = [0, 100]$ to see the results with combined sources of motion. Figure 2 shows the evolution of the maximum value of the stream function versus *Tm* for various *Ma*.

As we follow any curve for a given *Ma*, below a certain $Tm = Tm_1$ there is no effect of the RMF. This simply implies that the flow is dominated by Marangoni convection.

Also as *Ma* gets larger, Tm_1 needs to be larger for the RMF to modify the flow. At the other extreme, for any *Ma* there is a large enough $Tm = Tm_2$ where the curve merges with the $Ma = 0$ curve, which relates to the fact that the flow is then strongly dominated by the RMF. The most interesting region is certainly $Tm = [Tm_1, Tm_2]$ where both effects are playing a role. While the behavior of ψ_{max} for $Tm < Tm_1$ or $Tm > Tm_2$ is no surprise, the fact that ψ_{max} decreases before merging with the $Ma = 0$ curve was unexpected at first since both contributions to the meridional flow are counterclockwise and might therefore increase ψ_{max}. We present in figure 3, contours of ψ and u_θ for the three different *Tm* for $Ma = 100$ and $Pr = 0.02$.

The case $Tm = 100$, illustrates the Marangoni dominated flow and we find no significant decrease of ψ_{max} from the case without RMF where $\psi_{max} = 28.30$. Here Γ is a passive scalar. The weak angular momentum is strongly convected by the Marangoni convection which explains why the peak value of $u_\theta = 3.19$ is not at $r = 1, z = 0$ as one would find if $Ma = 0$. In such a case, the peak value would have been $u_\theta = 22.0$. The Marangoni flow increases the dissipation of Γ by forcing it toward the cold corner away from its source.

For $Tm = 10^4$, we still find that Γ is convected by the Marangoni flow, the maximum value $u_\theta = 230$ would have been 404 and located at $r = 1, z = 0$ if $Ma = 0$. The angular momentum is now large enough to be a source term in the vorticity equation. The strong axial gradient of angular momentum in the region $r > 0.5$ and $0.5 < z < 0.75$ would drive a clockwise cell if it was the only source of motion. Here it only opposes the Marangoni flow. This action could be compensated by the even stronger axial variation of angular momentum in $r > 0.5$ and $z > 0.75$ region that should increase the counterclockwise circulation but this axial variation takes place in a viscosity dominated region and turns out to have little effect. In the region $r < 0.5, z < 0.5$, there is a clear tendency to bidimensionality with strong z-independent angular momentum and the meridional motion is damped. This is a consequence of a Taylor-column effect. The maximum of ψ is then shifted toward the cold corner away from the bidimensional region.

For $Tm = 5 \cdot 10^5$, the flow is totally dominated by the RMF. We find the structure of a well defined core region where the angular momentum is z-independent and a spatially oscillating Bödewadt layer for $z > 0.9$ approximately. The Marangoni convection does not prevent the flow from achieving high angular momentum. This regime is well described in [9]. Here $\psi_{max} = 19.6$ but this value must be taken cautiously because the grid is too coarse near the top wall. It is important to notice also that the maximum value of ψ is fairly close to the top wall so that even if the ψ_{max} is lower than the value found in the Marangoni dominated case, the value of the radial velocity along the solidification front is much higher when the RMF dominates.

We can try to roughly estimate the relationship between *Ma*, *Pr* and *Tm* for which the transition from a Marangoni dominated to a RMF dominated flow will occur. A similar situation has been analyzed in [10] with the notable exception that the meridional flow is driven by a body force f_m distributed throughout the volume rather than by surface forces. In such case, for a sufficiently large Reynolds number flow, the criterion to have a dominant azimuthal motion is that $I_\theta > Re^{-1} I_m$, where *Re* is the effective Reynolds number based on the maximum value of the meridional flow, I_θ and I_m are some scaling for the azimuthal and meridional forcing. In fact, we found that the above criterion seems to be inappropriate to predict correctly the transition for the present configuration.

As long as the temperature along the free surface is not varying, the vorticity is prescribed at $r = 1$. For $Ma = 100$ with no azimuthal forcing, the maximum of the temperature has decreased to $T_{max} = 0.88$. This variation is small and probably unimportant. We then use the diffusive temperature distribution, to scale the surface force applied at

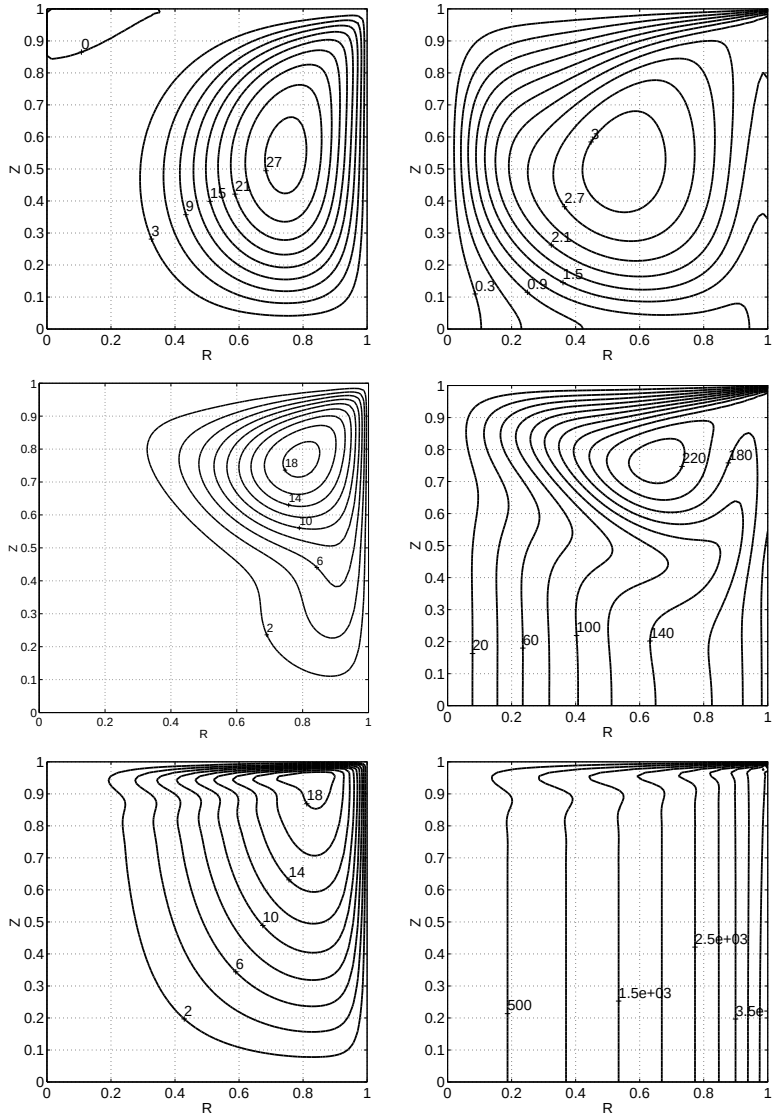

Figure 3: Contours of ψ and u_θ (left and right) for $Ma = 100$ and $Pr = 0.02$. From top to bottom $Tm = 100, 10^4$ and $5 \cdot 10^5$

$r = 1$ with

$$I_m = -\frac{Ma}{Pr}\int_0^1 \frac{\partial T}{\partial z}\, 2\pi \cdot 1 \cdot \mathrm{dz} \sim \frac{Ma}{Pr}\, 6.7. \tag{6}$$

Similarly, we scale the azimuthal body force by

$$I_\theta = Tm \int_0^1 \int_0^1 f_\theta\, 2\pi\, r\, \mathrm{dr}\, \mathrm{dz} \sim Tm\ 1.0. \tag{7}$$

We can define approximately Tm_c where the flow is dominated by azimuthal motion with the value of *Tm* when ψ_{max} is minimum. We then get the following values $Tm_c = 3.1 \cdot 10^3, 3.0 \cdot 10^4, 7.5 \cdot 10^4, 5.5 \cdot 10^5$ for $Ma = 10, 50, 100, 600$. The results obtained for $Ma = 600$ are not represented in figure 2 and are probably crude with our grid resolution but qualitatively correct. As *Ma* varies from 10 to 600, we find that *Re* varies from 80 to 1400. Interestingly, $I_m = I_\theta$ gives $3.3 \cdot 10^3, 1.6 \cdot 10^4, 3.3 \cdot 10^4, 2.0 \cdot 10^5$ which is a simple but reasonable estimate for Tm_c.

The key difference between the volume and surface forces can be understood by the following argument. As stated in [10], when the meridional forces are distributed in the volume, there is a redistribution of the angular momentum such that $\partial(\Gamma^2/r^3)/\partial z$ compensates $(\nabla \times f_m)_\theta$ in the vorticity equation, so that the azimuthal vorticity is everywhere smaller with the azimuthal body force than it is with only the meridional body force. In the present problem, azimuthal vorticity is produced by surface forces and its magnitude at the free surface is essentially the same for any *Tm*. Now there is a redistribution of the angular momentum such that $\partial(\Gamma^2/r^3)/\partial z$ opposes the diffusion and convection of azimuthal vorticity from the free surface to the interior.

3. Conclusions This study shows that an axisymmetric, Maragoni driven flow is affected by a RMF when both meridional and azimuthal forcing are broadly of the same order of magnitude. The important changes in a crystal grown by Float-Zone with an RMF are occurring in a range $Tm \sim 10^4$ for $Ma \sim 3000$ [1]. Thus a much weaker RMF than what would be predicted in this work affect the microsegregation distribution in the crystal produced. This supports the idea that the axisymmetric hypothesis is too restrictive and that a better understanding of the stability of such a base flow with respect to azimuthal and time dependence is needed.

Acknowledgements We wish to thank Daniel Henry of L'Ecole Centrale de Lyon who helped us setting up the continuation method. This research was supported by the US National Aeronautics and Space Administration under Grant NAG 8–1453.

REFERENCES

1. P. DOLD AND K. BENZ. Rotating magnetic fields: fluid flow and crystal growth applications. *Prog. Crys. Growth and Charact. of Mat.*, vol. 38 (1999), no. 1–4, pp. 7–38.
2. M. WANSCHURA, V. M. SHEVTSOVA, H. C. KUHLMANN, AND H. J. RATH. Convective instability mechanisms in thermocapillary liquid bridges. *Phys. Fluids*, vol. 7 (1995), no. 5, pp. 912–925.
3. G. CHEN, A. LIZÉE, AND B. ROUX. Bifurcation analysis of the thermocapillary convection in cylindrical liquid bridges. *J. Cryst. Growth*, vol. 180 (1997), no. 3–4, pp. 638–647.
4. N. KOBAYASHI. Computer simulation of the steady flow in a cylindrical floating zone under low gravity. *J. Cryst. Growth*, vol. 66 (1984), pp. 63–72.
5. E. CHÉNIER, C. DELCARTE, AND G. LABROSSE. Stability of the axisymmetric buoyant-capillary flows in a laterally heated liquid bridge. *Phys. Fluids*, vol. 11 (1999), no. 3, pp. 527–541.

6. T. KAISER AND K. W. BENZ. Floating-zone growth of silicon in magnetic fields III. numerical simulation. *J. Cryst. Growth*, vol. 183 (1998), no. 4, pp. 564–572.

7. P. MARTY, ET AL. On the stability of rotating mhd flow. In A. ALEMANY, P. MARTY, AND J. THIBAULT, editors, *Transfer Phenomena in Magnetohydrodynamic and Electroconducting Flows*, vol. 51 of *Fluid Mechanics and its Applications* (Kluwer Academic, 1999) pp. 327–343.

8. J. PRIEDE. Theoretical study of a flow in an axisymmetric cavity of finite length, driven by a rotating magnetic field. Ph.D. thesis, Institute of Physics, Latvian Academy of Science, Salaspils, 1993.

9. P. A. DAVIDSON. Swirling flow in an axisymmetric cavity of arbitrary profile, driven by a rotating magnetic field. *J. Fluid Mech.*, vol. 245 (1992), pp. 669–699.

10. P. A. DAVIDSON, ET AL. The role of Ekman pumping and the dominance of swirl in confined flows driven by Lorentz forces. *Eur. J. Mech.* B*/Fluids*, vol. 18 (1999), no. 4, pp. 693–711.

Received 01.02.2001